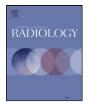
Contents lists available at SciVerse ScienceDirect





European Journal of Radiology

journal homepage: www.elsevier.com/locate/ejrad

Imaging study of ossifying fibroma with associated aneurysmal bone cyst in the paranasal sinus

B.T. Yang*, Y.Z. Wang¹, X.Y. Wang¹, Z.C. Wang²

Department of Radiology, Beijing Tongren Hospital, Capital Medical University, No. 1, Dongjiaominxiang, Dongcheng District, Beijing 100730, China

ARTICLE INFO

ABSTRACT

Article history: Received 10 November 2011 Received in revised form 4 April 2012 Accepted 5 May 2012

Keywords: Sinonasal cavity Ossifying fibroma Aneurysmal bone cyst CT MR imaging *Objective:* To determine the CT and MR imaging features of ossifying fibroma with aneurysmal bone cyst of the paranasal sinus.

Materials and methods: We retrospectively reviewed 15 patients with histopathology-proven ossifying fibromas with aneurysmal bone cysts in the paranasal sinus. All 15 patients underwent CT and MR imaging. The following imaging features were reviewed: location, shape, margin, CT findings, and MR imaging appearances and time-intensity curve of dynamic contrast-enhanced MR imaging.

Results: Ossifying fibromas occurred in the maxillary sinus in one patient, sphenoid sinus in 2, frontal sinus in 3, frontoethmoid sinuses in 3, and ethmoid sinus in 6 patients. Ossifying fibromas showed an elliptic-shape and aneurysmal bone cysts revealed a multicystic appearance, with well-demarcated margins. On unenhanced CT, ossifying fibromas appeared isodense to gray matter with scattered calcifications in nine, ground-glass appearance in 6 patients and aneurysmal bone cysts showed mixed density. Ossifying fibromas appeared isointense to gray matter in 12 and slightly hypointense in three patients on T1-weighted images, and isointense in 4 and hypointense in eleven patients on T2-weighted images, with moderate or marked enhancement after administration of contrast material. The time-intensity curves of eight ossifying fibromas exhibited a rapidly enhancing and rapid washout pattern. The intracystic components of aneurysmal bone cysts showed heterogeneous signal intensity on MR images, with fluid–fluid levels identified clearly by T2-weighted images, with marked enhancement.

Conclusions: Fluid–fluid levels within an elliptic-shape mass with scattered calcifications or ground-glass appearance is highly suggestive of this complicated entity in the paranasal sinus.

© 2012 Elsevier Ireland Ltd. All rights reserved.

1. Introduction

Ossifying fibroma (OF) is a benign fibro-osseous tumor characterized by the replacement of normal bone by a fibrous cellular stroma containing foci of mineralization. It is divided into three patterns of conventional OF (COF), juvenile psammomatoid OF (JPOF), and juvenile trabecular OF (JTOF) and arises most commonly in the mandible, followed by the maxilla and paranasal sinus [1]. Aneurysmal bone cyst (ABC) is a benign, tumor-like bone lesion developing mainly in the long bones and spine. It consists of multiple bloodfilled spaces of variable size that are separated by connective tissue. Only 3% ABCs occur in the head and neck region with mandible being the most common site [2]. Although OFs and ABCs have been extensively written up over the years, OF with associated ABC in the paranasal sinus is rare and, to date, only 7 cases have been reported in the literature [3–8]. We encountered 15 patients with histopathology – confirmed OF with ABC in the region over an 11year period and elaborately retrospectively reviewed their CT and MR imaging findings. Knowledge of the imaging characteristics can help to increase the awareness of this complicated entity among both clinicians and radiologists.

2. Materials and methods

2.1. Patients

This study was approved by the institutional review board. A retrospective review of 438 patients with totally excised and histopathology-proven sinonasal OFs over an 11-year period (May 2000 and April 2011) showed 15 (3.42%) OFs with associated ABC. There were 11 (73.3%) males and 4 (26.7%) females. The average age at diagnosis was 19.5 years (range 2–71 years). All 15 patients underwent surgical removal of these lesions by endoscopic sinus

^{*} Corresponding author. Tel.: +86 010 58268064; fax: +86 010 65131244. E-mail addresses: cjr.yangbenta@vip.163.com (B.T. Yang),

yzwang1981@163.com (Y.Z. Wang), juanjuan0824@163.com (X.Y. Wang), cjr.wzhch@vip.163.com (Z.C. Wang).

¹ Tel.: +86 010 58268064; fax: +86 010 65131244.

² Tel.: +86 010 58268071; fax: +86 010 65131244.

⁰⁷²⁰⁻⁰⁴⁸X/\$ - see front matter © 2012 Elsevier Ireland Ltd. All rights reserved. http://dx.doi.org/10.1016/j.ejrad.2012.05.010

surgery (ESS). The clinical presentations, surgical findings, and histopathologic diagnosis were extracted from the medical records.

2.2. CT technique

All 15 patients underwent unenhanced paranasal sinus CT. Images were obtained in both the axial and coronal planes using a Siemens Somatom Plus 4 (Siemens, Healthcare, Germany), Light-speed 16-slice (GE, Healthcare, Beijing, China) or Brilliance 64-slice CT system (Philips Healthcare, Best, the Netherlands). The imaging parameters are as follows: voltage 120 kV, current 200 mA, matrix 512 \times 512, section thickness 2 mm. Three patients were directly scanned in both planes and other 12 patients were scanned in the axial plane then reformatted from the superior wall of the frontal sinus to the inferior wall of the maxillary sinus on the axial plane and from the anterior wall of the frontal sinus to the posterior wall of the sphenoid sinus on the coronal plane. Images were reconstructed using both bone algorithm (window width 2000 HU, window level 200 HU) and soft tissue algorithm (window width 400 HU, window level 40 HU).

2.3. MR imaging technique

All 15 patients underwent paranasal sinus MR imaging prior to surgery. The MR examinations were performed on a 0.5 T unit (TOSHIBA Flexart, Japan) in one patient with a head coil and a 1.5 T unit MR system (GE, Healthcare, Milwaukee, WI, USA) in 14 patients with an 8-channels head coil. Fast spin-echo (FSE) pulse sequences were used in these patients. All 15 patients underwent pre- (T1WI and T2WI) and post-enhanced T1WI in the axial, coronal and sagittal planes. In addition, frequency-selective fat saturation technique was applied in the axial or coronal plane on post-enhanced T1WI. The imaging parameters are as follows: T1WI: repetition time (TR) 500–600 ms/echo time (TE) 10–15 ms; T2WI: TR 3000–3500 ms/TE 120–130 ms; excitations 2–4; echo train length 11–27; matrix 256×256 ; field of view of (FOV) 20 cm \times 20 cm; and section thickness 4–5 mm, intersection gap 0–0.5 mm.

Rapid manual bolus intravenous injection (2 mL/s) of 0.1 mmol of Gadopentetate dimeglumine (Magnevist; Schering, Germany) per kilogram of body weight and followed by a 10-mL flush of normal saline solution. Dynamic contrast-enhanced (DCE) MR imaging was performed in the axial or coronal plane by using 3D fast spoiled gradient echo (FSPGR) before conventional post-contrast T1WI in 8 patients. The following scan parameters: TR 8.4 ms, TE 4.0 ms; excitation 1; matrix 256×160 ; FOV $20 \text{ cm} \times 20 \text{ cm}$; and section thickness 3.2 mm, intersection gap 0 mm. A total twelve sets of dynamic images were obtained. Each set included six images and needed 13 s. The interset time gap was 12 s. The whole dynamic series took 5 min in total. After the dynamic scan, source images were transferred to a GE AW 4.2 workstation (GE Healthcare) for further analysis. In the largest solid enhancing portion of the tumors, authors manually drew regions of interest (ROI) for signal intensity measurement. ROI was approximately 3 mm in diameter. In order to ensure the accuracy of TIC, several ROI were chosen on basis of the lesion size and subsequently compared with their histopathology. At the same time, the change in signal intensity of a similar ROI placed on the masseter muscle was used for reference.

2.4. Image analysis

The CT and MR images were evaluated by three experienced radiologists and the findings were reached by consensus.

In the present study, we adopt the classification of timeintensity curve (TIC) of DCE MR imaging proposed by Yabuuchi et al. [9,10]: (1) Type I (steady enhancement pattern) appears as a straight or curved line, enhancement continues over the entire dynamic study; (2) Type II (rapidly enhancing and slow washout pattern) appears as growing enhancement at early stage and then has a sharp bend to form a plateau at middle and later stages [T_{peak} (early peak time) < 60 s, 10% \leq WR (washout ratio) < 20%]; and (3) Type III (rapidly enhancing and rapid washout pattern) appears as growing enhancement during the early stage and then progressively decrease in signal intensity ($T_{\text{peak}} < 60$ s, WR \geq 20%).

3. Result

The most common symptoms were nasal obstruction (15 patients, 100%), rhinorrhea (12 patients, 80%), proptosis (12 patients, 80%), diplopia (9 patients, 60%), decreased visual acuity (6 patients, 40%), headache (6 patients, 40%), epistaxis (5 patients, 33.3%), and dysosmia (3 patients, 20%).

After excision of 15 masses, histopathological examinations demonstrated COF in 10 (66.7%), JPOF in 4 (26.7%) patients, and JTOF in one patient (6.7%). ABCs were found within the 15 OFs as well. OFs originated from the maxillary sinus in one patient (6.7%), sphenoid sinus in 2 (13.3%), frontal sinus in 3 (20%), frontoethmoid sinuses (anterior ethmoid sinus and frontal sinus) in 3 (20%), and ethmoid sinus in 6 patients (40%).

OFs showed elliptic-shape and had well-defined margins. The mean maximum diameter was 48 mm (range 28–83 mm). Associated ABCs occupying at least one half of the total volume of OFs were found in 12 patients (80%), of which 3 almost occupied the whole OFs. The ABCs revealed multicystic appearance and had well-demarcated margins. The mean maximum diameter was 30 mm (range 16–72 mm).

On non-enhanced CT, OFs appeared isodense to gray matter with scattered calcifications in nine (60%) and ground-glass density in six (40%) patients (Figs. 1 and 2A). Associated ABCs showed an expansile, multicystic mass with mixed attenuation (Figs. 1 and 2A). Fluid–fluid levels were noted in 6 patients (40%). All the lesions caused the surrounding bony expansion and displacement, of which 5 also had bony erosion, including 3 JPOFs and 2 COFs.

OFs appeared isointense relative to gray matter in 12 (80%) and slightly hypointense in 3 patients (20%) on T1-weighted images (Figs. 1 and 2B), and isointense in 4 (26.7%) and hypointense in 11 patients (73.3%) on T2-weighted images (Figs. 1 and 2C), with moderate or marked enhancement after administration of contrast material (Fig. 1D). The TICs of 8 OFs revealed a rapidly enhancing and rapid washout pattern, which were consistent with Type III on the basis of the classification proposed by Yabuuchi (Fig. 1E and F).

The intracyst component of ABCs showed heterogeneous signal intensity on MR images, especially on T2-weighted images, with fluid–fluid levels separated by septa, without enhancement (Figs. 3 and 4). The prevalence of fluid–fluid levels of T1-, T2-, and enhanced T1-weighted images were 53.3% (8/15), 100% (15/15) and 100% (15/15), respectively. Fluid–fluid levels were optimally demonstrated on axial or sagittal orientation. The periphery and septa appeared isointense on MR images, with marked enhancement (Figs. 3 and 4).

The following features are also noted, especially on MR imaging: (a) proptosis and compression of extraocular muscle (12 patients, 80%), (b) compression of adjacent brain tissue and with slight reactive meningeal thickening (9 patients, 60%), and (c) protrusion into pterygopalatine fossa and infratemporal fossa (3 patients, 20%).

Regular follow-up of 15 patients for 0.5–10 years following surgery, two patients recurred within the first year of the initial treatment and other 13 patients recovered well. These two patients subsequently underwent complete local excision operation, respectively. After second operation, no evidence of Download English Version:

https://daneshyari.com/en/article/6244342

Download Persian Version:

https://daneshyari.com/article/6244342

Daneshyari.com